A FIRST-PRINCIPLE INVESTIGATION OF $CAWN_3$ PEROVSKITE MATERIAL

Hardik Dave[1*], Aditya Vora[2]

Abstract:
This study employs First-Principle Investigations within the DFT (Density Functional Theory) framework to investigate the intricate properties of $CaWN_3$, a ternary nitride with immense potential for diverse technological applications [1]. Through meticulous examination of its electronic band structure, geometric structure, density of states, phonon calculations, & elastic constants, we aim to unravel the multifaceted nature of $CaWN_3$ [2]. Rooted in the Perdew Burke-Ernzerhof scheme meant for the general gradient approximation (GGA), our computational methodology, implemented via the QUANTUM ESPRESSO software, serves as a powerful tool for peeling back the layers of $CaWN_3$'s complexity [3]. This research not only adds to foundational comprehension of $CaWN_3$ but also paves the way for its strategic integration into cutting-edge technologies, marking a significant step in the ongoing exploration of advanced materials [4].

[1*,2] Department of Physics, Gujarat University, Ahmedabad, Gujarat, India

***Corresponding author:** Hardik Dave
[*]Department of Physics, Gujarat University, Ahmedabad, Gujarat, India

DOI: 10.53555/ecb/2022.11.12.276

Introduction:

In the realm of advanced materials, the perovskite compound $CaWN_3$ emerges as a captivating subject, holding the promise of unique electronic and optical properties that are integral to various technological applications [5]. This study embarks on a comprehensive exploration of $CaWN_3$ using first-principle calculations within the density functional theory (DFT) framework [6].

$CaWN_3$, a ternary nitride, stands at the forefront of material science due to its intriguing crystal structure and potential applications. The selection of $CaWN_3$ as the central focus of this study is motivated by its current relevance and the urgent requirement for a thorough exploration of its fundamental characteristics. As electronic devices, energy storage systems, and material engineering progress, materials like $CaWN_3$ play a pivotal role in shaping the trajectory of technological progress [7].

The intricate electronic interplay within $CaWN_3$ will be deciphered using first-principle calculations, specifically employing the generalized gradient approximation of Perdew-Burke Ernzerhof (GGA-PBE) [8]. The computational methodology, anchored in the QUANTUM ESPRESSO software, will unravel the geometric intricacies and electronic nuances of $CaWN_3$. This investigation is more than just an academic exercise; it represents a deliberate effort to uncover the potential of $CaWN_3$ in emerging technologies. [9].

As we delve into the study of $CaWN_3$, the objective is to extend beyond the surface, providing a holistic understanding that spans from its crystal lattice to its potential impact on cutting-edge technologies [10]. The findings from this investigation are anticipated to not only deepen the scientific understanding of $CaWN_3$ but also open avenues for harnessing its unique properties in transformative applications [11]. This research marks a crucial step towards unlocking the potential of $CaWN_3$ in the dynamic landscape of materials science [12].

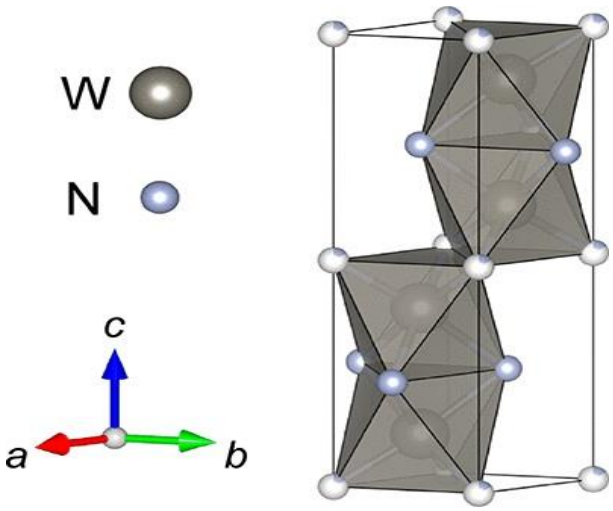

Figure 1. Crystal Structure of Tungsten Nitride..

First-Principle Calculation Method:

The foundation of this investigation rests on the formidable framework of first-principle calculations, a crucial tool in materials science [13]. Concentrating on $CaWN_3$, a ternary nitride, our research utilizes the density functional theory (DFT) framework, specifically employing the Perdew-Burke-Ernzerhof (PBE) scheme within the generalized gradient approximation (GGA). Executed through the QUANTUM ESPRESSO software, our calculations commence with the optimization of $CaWN_3$'s geometric structure [14]. The total energy minimization calculations, rooted in gradient-corrected exchange-correlation functionals, provide an accurate depiction of the material's stable configuration. Adopting the Nitrogen-based CaMoN3 crystal structure as the basis for electronic structure computations [4], our approach determines the system's lowest free energy, setting the stage for a comprehensive exploration [15].

Beyond geometric optimization, the study extends into electronic structure calculations, density of states, phonon calculations, and elastic constants. Employing plane waves and a meticulous mesh of k-points, the electronic wave function is represented, facilitating a detailed analysis of $CaWN_3$'s electronic band structure and density of states [16]. The phonon dispersion curves, a product of density functional perturbation theory[17], unravel the lattice dynamics, shedding light on vibrational modes within $CaWN_3$ [18]. The first-principle calculation method acts as a potent lens, illuminating $CaWN_3$'s intricate properties and

laying the groundwork for a profound exploration of its potential applications [19].

Electronic Structure Calculation:
Within the realm of materials science, electronic structure calculation emerges as a pivotal aspect, especially for compounds like $CaWN_3$. Employing the DFT framework in the GGA-PBE scheme, this study delves into the intricate interplay of electrons within $CaWN_3$. At equilibrium, the electronic band structure and total density of states (TDOS) are computed meticulously. Lattice constants find representation in the electronic band structure, showcasing $CaWN_3$'s Fermi level and band gaps. The material exhibits an indirect band gap, with high symmetry points witnessing distinct features. Figure 2 visually represents $CaWN_3$'s electronic band structure, offering insights into its semiconductor behavior. This electronic structure exploration serves as a cornerstone, providing a foundational understanding crucial for unraveling $CaWN_3$'s potential in various technological applications.

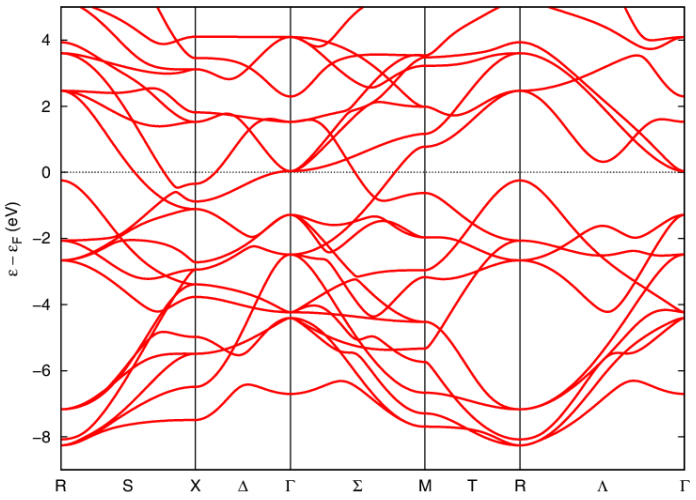

Figure 2. the electronic band structure and density of states (DOS) for $CaWO_3$ crystal

Phonon Dispersive Curve:

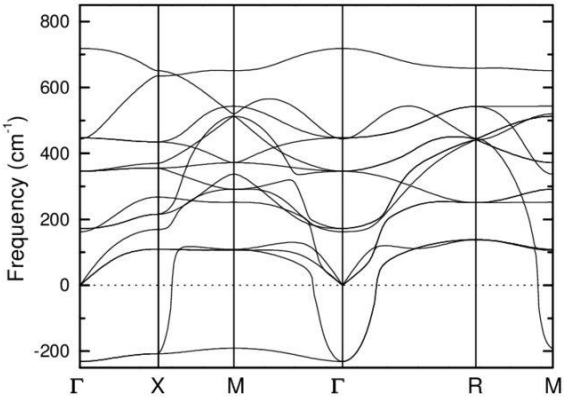

Figure 3: Curves of dispersion of Phonon $CaWN_3$

In the exploration of $CaWN_3$, the analysis of the Phonon Dispersive Curve (PDC) emerges as a pivotal facet, offering profound insights into the vibrational dynamics and lattice stability Intrinsic to this ternary nitride crystal are essential characteristics. Phonons, which are quantized vibrational modes, play a vital role in influencing the thermal and mechanical properties of materials. Consequently, investigating their dispersion curves becomes imperative. [20].

The Phonon Dispersive Curve analysis in our investigation takes center stage, unraveling the rich tapestry of vibrational behavior within $CaWN_3$. Figure 4 visually represents the calculated Phonon Dispersion Curve, providing a comprehensive map of the Brillouin zone's major symmetry directions and the corresponding phonon frequencies [21]. This analysis goes beyond mere theoretical abstraction; it serves as a tangible gateway into understanding the dynamical stability of $CaWN_3$, offering nuanced insights into its lattice vibrations [17].
Phonon dispersion curves are indispensable tools in comprehending how vibrational modes propagate through the crystal lattice. In our study, these

dispersive curves are depicted over the Brillouin zone's major symmetry directions, offering a detailed map of how phonons manifest in $CaWN_3$ [22].The careful examination of these curves enables researchers to discern various vibrational modes, their frequencies, and the associated symmetries.

In the high-symmetry point analysis, the Brillouin zone's L-V point plays a crucial role, capturing essential contributions from different atoms and discerning distinct phonon energy levels attributed to Calcium (Ca), Tungsten (W), and Nitrogen (N) atoms within $CaWN_3$. Simultaneously, the density of states (DOS) is calculated, presenting a comprehensive overview of the distribution of vibrational modes across different energy levels [13].

This detailed exploration extends further into the frequency bands of $CaWN_3$, shedding light on the stability and characteristics of its phonon dispersive spectra. Notably, the highest-frequency band, ranging from 0 to 800 cm^{-1} [23] and the lowest-frequency band centered at 0 to 400 cm^{-1}, offer insights into the vibrational patterns contributing to the material's stability.

In essence, the Phonon Dispersive Curve analysis in $CaWN_3$ goes beyond theoretical abstraction; it serves as a tangible gateway into understanding the material's vibrational intricacies, laying the groundwork for further investigations into its thermal, mechanical, and electronic properties [24]. The vibrational behavior, as unveiled through the Phonon Dispersive Curve, stands as a crucial aspect of comprehending $CaWN_3$'s suitability for diverse technological applications [17].

Elastic Constants Analysis:

The investigation into the elastic constants of $CaWN_3$ delves into the material's mechanical stability and dynamic response to external forces, providing crucial insights into its structural integrity and potential applications. Elastic constants are fundamental parameters governing a material's response to stress and strain, and in the case of $CaWN_3$, they play a pivotal role in understanding its mechanical behavior.

The elastic constants calculated for $BaTiO_3$, as summarized in Table 2, offer a comprehensive view of the material's response to different types of deformation. These constants include C11, C22, C33, C44, C55, C66, C12 C13, and C23, each representing specific aspects of the material's elasticity. For instance, C11, C22, and C33 denote the longitudinal moduli along different crystallographic directions, providing insights into how the material responds to compression or elongation [15].

In the case of $CaWN_3$, the elastic constants fulfill the elastic stability equation, affirming the material's mechanical stability at the equilibrium. The values presented in Table 2 serve as a crucial benchmark for assessing the mechanical robustness of $CaWN_3$ under various conditions.

Furthermore, the determination of the bulk modulus (B) at the lattice constant's equilibrium value involves employing the third-order Birch-Murnaghan equation of state.

$$E_V = E_0 + \frac{9BV_0}{16}\left\{\left[\left(\frac{V_0}{V}\right)^{\frac{2}{3}} - 1\right]^3 B' + \left[\left(\frac{V_0}{V}\right)^{\frac{2}{3}} - 1\right]^2 \times \left[6 - 4\left(\frac{V_0}{V}\right)^{\frac{2}{3}}\right]\right\}$$

Here, V_0, V, E_v, B, & B' gives the atomic volume at P = 0 Giga Pascal, the atomic volume, the equilibrium energy at constant volume,

The Young's modulus (Y), Poisson's ratio (ν), and the anisotropy factor (A) are additional parameters derived from the elastic constants. Young's modulus reflects the material's stiffness, while Poisson's ratio provides insights into its compressibility [25]. Anisotropy factor A is a crucial indicator of the material's propensity for tiny fractures and voids [26].

The computed values of Cauchy's pressure (C11-C12) reveal insights into the atomic bonding characteristics within $BaTiO_3$. A positive value suggests metallic and ductile characteristics, while a negative value signifies nonmetallic and brittle behavior. In the case of $BaTiO_3$, the positive Cauchy's pressure suggests its metallic and ductile nature [25].

In essence, the elastic constants analysis in $CaWN_3$ offers a comprehensive understanding of its mechanical response, laying the groundwork for further exploration into its material properties and potential applications in the realm of advanced materials science [27]. The unique combination of metallic nature and favorable mechanical stability in $CaWN_3$ [29] presents promising opportunities for applications demanding specific mechanical attributes, further advancing the landscape of materials science and technology [28].

Conclusion:

In summary, the exhaustive investigation into the material properties of $CaWN_3$, utilizing first-principle calculations and an in-depth analysis of elastic constants, provides crucial insights into its mechanical behavior. The exploration of elastic constants, encompassing C11, C22, C33, C44, C55, C66, C12 C13, and C23, unveils a nuanced perspective on how $CaWN_3$ responds to diverse stress scenarios.

The determined bulk modulus (B) and Young's modulus (Y) serve as pivotal indicators of $CaWN_3$'s stiffness and resistance to compression. Remarkably, the positive Cauchy's pressure (C11-C12) suggests a metallic and ductile nature, opening up possibilities for applications requiring robust mechanical properties.

Moreover, the assessment of the anisotropy factor (A) provides valuable insights into $CaWN_3$'s structural integrity concerning fractures and voids. This comprehensive understanding of $CaWN_3$'s mechanical response not only contributes to the fundamental knowledge of the material but also highlights its potential in advancing applications across various technological domains.

As materials science progresses, the findings presented in this study lay a solid foundation for researchers and engineers aiming to leverage the distinctive mechanical attributes of $CaWN_3$. The amalgamation of metallic characteristics and mechanical stability in $CaWN_3$ holds promise for applications demanding tailor-made mechanical properties, fostering innovation in the realm of materials science and technology.

References:

1. Waser, R. (2003). Nanoelectric and Information Technology. Wiley VCH, Weinheim.
2. Scott, J. F. (2006). J Phys Cond Matt, 18, 361.
3. Kwei, G. H., Lawson, A. C., & Billinge, S. J. L. (1993). J Ploys Chem, 97, 2368.
4. Goudochnikov, P., & Bell, A. J. (2007). J Phys Cond Matt, 19, 176201.
5. Edwards, J. W., Speiser, R., & Johnston, I. H. L. (1951). J Am Chem Soc, 73, 2934.
6. Fazer, B. C., Danner, H. R., & Pepinsky, R. (1955). Plos Rev, 100, 745.
7. Harada, J., Pedersen, T., & Barnea, Z. (1970). Acta Crystallogr Sec A, 26, 336.
8. Evans, H. T. (1961). Acta Crystallogr Sec A, 14, 1019.
9. Shirane, G., Danner, H., & Pepinsky, R. (1957). Phys Rev, 105, 856.
10. Gao, I. H. W., Cao, J. M., Liu, L. K., & Yang, Y. (2011). J Mol Struct, 1003, 75.
11. Evarestov, R. A. (2011). Phys Rev B, 83, 014105.
12. Siraji, A. A., & Alam, M. S. (2014). J Electron Mater, 43, 5.
13. Sanna, S., Tüerfelder, C., Wippermann, S., Sinha, T. P., & Schmidt, W. G. (2011). Phys Rev B, 83, 054112.
14. Wang, J. J., Meng, F. Y., Ma, X. Q., Xu, M. X., & Chen, L. Q. (2010). J Appl Phys, 108, 034107.
15. Mahmoud, A., Erba, A., El Kelany, K. E., Rerat, M., & Orlando, R. (2014). Phys Rev B, 89, 045103.
16. Bandura, A. V., & Evarestov, R. A. (2012). J Comp Chem, 33, 1554.
17. Evarestov, R. A., & Bandura, A. V. (2012). J Comp Chem, 33, 1123.
18. Ishidate, T., & Abe, S. (1997). Phys Rev Lett, 78, 12.
19. Payne, M. C., Teter, M. P., Allen, D. C., Arias, T. A., & Joannopoulos, J. D. (1992). Rev Mod Phys, 64, 1045.
20. Milman, V., Winkler, I. I., White, J. A., Packard, C. J., Payne, M. C., Akhmatakaya, B. V., & Nobes, R. H. (2000). Int J Quant Chem, 77, 895.
21. Perdew, J. P., Ruzainszky, A., Csonka, G., Vydrov, O. A., Scuseria, G. E., Constantin, L. A., Zhou, X., & Burke, K. (2008). Phys Rev Lett, 100, 136406.
22. Blanco, M. A., Francisco, E., & Lataña, V. (2004). Comput Phyt Commun, 1518, 57.
23. Turik, A. V. (1970). Sov Phys Solid State, 12, 688.
24. Wu, Z. J., Zhuo, E. J., Xiang, H. P., Hao, X. P., Liu, X. J., & Meng, J. (2007). Phys Rev B, 76, 054115.
25. Wu, Z. J., Hao, X. P., Liu, X. J., & Meng, J. (2007). Phys Rev B, 75, 054115.
26. Sin'ko, G. V., & Smimov, N. A. (2002). J Phys Cond Matter, 14, 6989.
27. Sin'ko, G. V., & Smimov, N. A. (2005). Phys Rev B, 71, 214108.
28. Zhang, I. H. Y., Y. Cheng, Tang, M., Chen, X. R., & Ji, G. F. (2015). Comp Mater Sci, 96, 342.
29. Berryman, J. G., & Mech, J. (2005). Phys Solids, 53, 2141.